HHS Public Access

Author manuscript

Exp Neurol. Author manuscript; available in PMC 2016 November 01.

Published in final edited form as:

Exp Neurol. 2015 November ; 273: 151–160. doi:10.1016/j.expneurol.2015.08.008.

Combination Therapy with Lenalidomide and Nanoceria Ameliorates CNS Autoimmunity

Erez Eitan[1], **Emmette R. Hutchison**[1], **Nigel H. Greig**[2], **David Tweedie**[2], **Hasan Celik**[3], **Soumita Ghosh**[3], **Kenneth W. Fishbein**[3], **Richard G. Spencer**[3], **Carl Y. Sasaki**[5], **Paritosh Ghosh**[5], **Soumen Das**[4], **Susheela Chigurapati**[6], **James Raymick**[7], **Sumit Sarkar**[7], **Srinivasulu Chigurupati**[7], **Sudipta Seal**[8], and **Mark P. Mattson**[1,9,*]

[1]Laboratory of Neurosciences, National Institute on Aging Intramural Research Program, Baltimore, MD 21224.

[2]Translational Gerontology Branch, National Institute on Aging Intramural Research Program, Baltimore, MD 21224.

[3]Laboratory of Clinical Investigation, National Institute on Aging Intramural Research Program, Baltimore, MD 21224.

[4]Material Science and Engineering College of Medicine, University of Central Florida, Orlando, Florida 32816.

[5] Laboratory of Immunology, National Institute on Aging Intramural Research Program, Baltimore, MD 21224

[6]Arkansas Regional Laboratory, Office of Regulatory Affairs, U.S. Food and Drug Administration, 3900 NCTR Road, Building 26, Jefferson, AR 72079, USA

[7]Division of Neurotoxicology, National Center for Toxicological Research/FDA, Jefferson, AR 72079.

[8]Advanced Materials Processing and Analysis Centre, Nanoscience Technology Center, Mechanical Materials Aerospace Engineering, University of Central Florida, Orlando, Florida 32816.

[9]Department of Neuroscience, Johns Hopkins University School of Medicine, Baltimore, MD 21205.

Abstract

Objective—Multiple sclerosis (MS) is a debilitating neurological disorder involving an autoimmune reaction to oligodendrocytes and degeneration of the axons they ensheath in the CNS.

*Correspondence: mark.mattson@nih.gov; Phone – 410 558 8463..

Authorship: E.E., N.H.G., K.W.F., S.S. and M.P.M. conceived the study and designed the experiments. E.E., E.R.H., D.T., H.C., S.G., S.D., S.C. and S.C. performed the experiments. E.E., N.H.G., K.W.F., S.D., S.S. and M.P.M. wrote the manuscript.

Because the damage to oligodendrocytes and axons involves local inflammation and associated oxidative stress, we tested the therapeutic efficacy of combined treatment with a potent anti-inflammatory thalidomide analog (lenalidomide) and novel synthetic anti-oxidant cerium oxide nanoparticles (nanoceria) in the experimental autoimmune encephalomyelitis (EAE) mouse model of MS.

Methods—C57BL/6 mice were randomly assigned to a control (no EAE) group, or one of four myelin oligodendrocyte glycoprotein-induced EAE groups: vehicle, lenalidomide, nanoceria, or lenalidomide plus nanoceria. During a 23 day period, clinical EAE symptoms were evaluated daily, and MRI brain scans were performed at 11-13 days and 20-22 days. Histological and biochemical analyses of brain tissue samples were performed to quantify myelin loss and local inflammation.

Results—Lenalidomide treatment alone delayed symptom onset, while nanoceria treatment had no effect on symptom onset or severity, but did promote recovery; lenalidomide and nanoceria each significantly attenuated white matter pathology and associated inflammation. Combined treatment with lenalidomide and nanoceria resulted in a near elimination of EAE symptoms, and reduced white matter pathology and inflammatory cell responses to a much greater extent than either treatment alone.

Interpretation—By suppressing inflammation and oxidative stress, combined treatment with lenalidomide and nanoceria can reduce demyelination and associated neurological symptoms in EAE mice. Our preclinical data suggest a potential application of this combination therapy in MS.

Introduction

Multiple sclerosis (MS) is a common autoimmune neurological disorder typically diagnosed in people between the ages of 20 and 40 years; the symptoms include impaired sensory and motor function, autonomic dysfunction and cognitive impairment. Most MS patients exhibit a relapsing and remitting disease course, while others experience a more severe progressive disease leading to death (Calabresi, 2004, Goldenberg, 2012, Friese et al., 2014). While the causes of MS are unclear, the mechanism of its progression involves an autoimmune reaction to antigens on oligodendrocytes that myelinate axons in the brain and spinal cord, resulting in dysfunction and damage to the axons (Lassmann et al., 2012). The disease etiology includes the activation of autoreactive Th1 cells and Th17 cells with T-cell receptors (TCR) that recognize myelin proteins (Greer, 2013). The T-cells infiltrate the brain and spinal cord parenchyma where they induce local inflammation that involves activation of microglia, astrocytes and infiltration of blood-derived macrophages (Jack et al., 2005, Hauser and Oksenberg, 2006). This local immune response damages myelin and axons resulting in white matter lesions that can be visualized by MRI (Calabresi, 2004).

While there is no cure for MS, many patients benefit from drugs that suppress the immune response and reduce the frequency and severity of disease relapse periods; such treatments include interferons and glatiramer acetate. However, these treatments are not effective in many patients and may not prevent axon damage or promote remyelination (Goldenberg, 2012, Carrithers, 2014). Additional treatments that reduce white matter damage and slow or reverse the disease processes are therefore needed. The thalidomide derivative lenalidomide

is used for the treatment of multiple myeloma and several myelodysplastic syndromes; it is a potent inhibitor of tumor necrosis factor (TNF) production (Bartlett et al., 2004). Lenalidomide also increases the production of interferon-γ, IL-10 and IL-2, and modulates natural killer cell and antibody-dependent cellular cytotoxicity (Kotla et al., 2009, Zhu et al., 2013). While clinical trials of thalidomide or lenalidomide in MS patients have not been performed, thalidomide was reported to reduce inflammation and delay symptom onset in an experimental autoimmune encephalomyelitis (EAE) animal model (Sastry, 1999, Contino-Pepin et al., 2009, Contino-Pepin et al., 2010, Correa et al., 2010). Although lenalidomide treatment has not previously been tested in the EAE model, it has been reported to attenuate degeneration of motor neurons in a mouse model of amyotrophic lateral sclerosis (Neymotin et al., 2009).

Excessive cellular oxidative stress is evident in the white matter lesions of MS patients (Haider et al., 2011). Nanoceria nanoparticles have the unique capability to switch between Ce^{3+} and Ce^{4+} states and enable potent scavenging of reactive oxygen species (ROS) including nitric oxide (NO) (Das et al., 2013). Preclinical studies have demonstrated beneficial effects of nanoceria treatment in experimental models of several pathological conditions that involve oxidative stress, including dermal wounds, macular degeneration and Alzheimer's disease (Cimini et al., 2012, Dowding et al., 2012, Chigurupati et al., 2013, Dowding et al., 2014). ROS also play an important role in inflammation, and nanoceria can inhibit macrophage activation, promote T-cell differentiation into the Th2 phenotype and reduce demyelination in white matter injury animal models (Hirst et al., 2009, Schnen et al., 2013, heckman et al., 2013).

Here we report that combined treatment with lenalidomide and nanoceria is much more effective than either treatment alone in reducing white matter damage and neurological deficits in a mouse MS model. These results suggest that combination therapy with potent anti-inflammatory and antioxidant drugs might be effective in slowing or halting the disease process in MS.

Materials and Methods

EAE induction

Fifty 10 week-old female C57BL/6 mice (Charles River Laboratories) were maintained under a 12 h light/12 h dark cycle with food and water available ad libitum. All procedures were approved by the National Institute on Aging Animal Care and Use Committee and complied with NIH guidelines. After two weeks of acclimation to the animal facility, mice were randomly assigned to one of 5 groups: untreated (healthy) mice; vehicle-treated EAE mice; lenalidomide-treated EAE mice; nanoceria-treated EAE mice; and EAE mice treated with both lenalidomide and nanoceria (10 mice per group). One mouse in the vehicle-EAE group died on EAE day 4 and one mouse in the lenalidomide + nanoceria group died on EAE day 7; neither mouse had exhibited EAE symptoms prior to their death. EAE was induced with MOG 35-55 (Hooke Laboratories, Inc.; kit EK-2110). Briefly, on day 0, mice received two subcutaneous injections of MOG 35-55 peptide mix with adjuvant and 2 hours later pertussis toxin was injected intraperitoneally. One day later (experimental day 1) a second pertussis toxin injection was administered. The mice were evaluated daily for 23

days and soft food was placed in their cages when severe motor impairment occurred. The weight of each mouse was measured before EAE induction and on experimental days 5, 9, 17 and 23. A timeline for all procedures, including drug administration, magnetic resonance imaging and behavioral testing is shown in Figure 1A.

Lenalidomide and nanoceria preparation and treatment

Lenalidomide was synthesized in the laboratory of N.G. using methods similar to those described previously (Zhu et al., 2003), and was greater than 99% pure. Lenalidomide was dissolved in 1% carboxymethyl cellulose, 0.9% saline solution and was administered by intraperitoneal injection at a dose of 25 mg/kg. The solution was shaken for 15 min before first injection and throughout the injections. Cerium oxide nanoparticles (nanoceria) were synthesized using methods described previously (Karakoti et al., 2008). The size, uniformity and oxidation state of the nanoceria was evaluated by transmission electron microscopy, X-ray photon spectrometry and X-ray diffraction analyses. Nanoceria were suspended in phosphate-buffered saline (PBS) and administered in a dose of 1 mg/kg by intravenous injection.

Behavioral analysis

All mice were examined daily and a clinical score was assigned according to a widely-employed six-point scale as follows: 0) No evidence of motor impairment, tail is erect, and mouse spreads hind legs when picked up by the tail; 1) tail is limp when the mouse is picked up by the base of the tail; 2) limp tail, weakness in hind legs/wobbly gait, and legs closed when picked up by the tail; 3) limp tail with paralysis of one front and one hind limb; 4) limp tail, complete hind limb paralysis, and partial forelimb paralysis; 5) mouse is found dead or must be euthanized due to severe paralysis. Mice were tested on a rotarod apparatus (Med Associates Inc.) at baseline and on days 7 and 17 after EAE induction. Mice were tested twice each day. In the first trial, the mouse was placed on a rod rotating at 2.5 RPM and the speed was increased progressively to 25 RPM over a 5 minute period. In the second trial, the mouse was placed on a rod rotating at 4.0 RPM and the speed was increased progressively to 40 RPM over a 5 minute period.

In vivo MRI

MRI data were acquired on 6 randomly chosen mice per group using a Bruker Biospec 7T/30 cm scanner (Bruker Biospin MRI, Ettlingen, Germany) equipped with a Bruker 72 mm birdcage resonator configured as a transmit-only coil and a RAPID two-channel receive-only mouse head array coil (RAPID MRI International, Columbus, Ohio). Anesthesia was induced by inhalation of a 2.5% v/v mixture of isoflurane in oxygen and maintained during scanning by breathing a 1-2% mixture administered by mask. The exact concentration of isoflurane was continuously adjusted to maintain a respiration rate of 40-60 breaths per minute. The animal's vital signs were continuously monitored using an SA Instruments model 1025 MR-compatible physiological monitoring system (SA Instruments, Stony Brook, NY) equipped with pneumatic respiration and fiber optic temperature sensors. Body temperature was maintained during scanning by application of a stream of warm air supplied by an SA Instruments heating unit with rectal temperature feedback control. All the images were viewed and processed using Bruker ParaVision imaging software. The MRI images

were acquired during days 11-13 and again during days 20-22 after EAE induction. During each day of the 3-day imaging periods, 2 mice from each of the 5 groups were imaged. The imaging parameters for the multi-slice multi-echo experiments used were: repetition time TR=5000 ms , echo time TE=10 ms, FOV= 30 mm × 20 mm, matrix size 192 × 128, slice thickness = 1 mm, number of averages NA=2 and number of echoes ETL=32, resulting in an acquisition time of 21 min 20 s. A package of 12 contiguous coronal slices was placed such that the brain was scanned from the olfactory bulb to the brain stem with an in-plane resolution of 156 μm × 156 μm. The T2-maps were constructed by fitting the T2-weighted magnitude images to a 3-parameter mono-exponential model pixel by pixel. The ROI's for the volumetric measurement of the ventricles were drawn on the T2 maps, which exhibit greater contrast between CSF and brain parenchyma than is present in the raw T2-weighted images; Supplemental Figure 1 shows an example of a T2 map from one mouse brain.

Splenocyte culture and FACS analysis

Ten mice received two subcutaneous injections of MOG 35-55 peptide mixed with adjuvant and were then randomly assigned to two groups, one treated with lenalidomide and nanoceria, and the other with vehicle (1% carboxymethyl cellulose). Ten days later mice were euthanized, their spleens removed and weighted, and spleen tissue was processed to remove red blood cells using ACK lysis buffer (Gibco). Spleenocytes were isolated and directly processed for FACS analysis or cultured (10 million splenocytes) for 72 hours in the presence of MOG35-55 peptide (20 μg/ml, Anaspec) and IL-23 (20 ng/ml, R&D research). Lenalidomide and nanoceria were added to the splenocyte cultures from the mice treated with lenalidomide and nanoceria. Adherent cells were processed for immunoflourecence analysis and non-adherent cells were harvested and stained for flow cytometric analysis. For immunofluorescence staining of splenocytes, cells were grown on coverslips and then fixed with 4% paraformaldehyde in PBS for 20 minutes. The cells were washed with PBS and incubated in blocking solution containing 5% BSA for 30 minutes. Then the following antibodies were added: MHC II APC (BD Biosciences 17-5321-81), CD11c FITC (Biolegend 117306), CD86 PE (BD Biosciences 553692) and cells were incubated overnight. The cells were then washed with PBS, incubated in the presence of appropriate fluorescently tagged secondary antibodies, and then incubated with DAPI for 10 minutes and the coverslips were mounted on slides.

Immunohistochemistry

Mice were anesthetized 23 days post MOG injection with isoflurane prior to cardiac perfusion with 4% paraformaldehyde (PFA). Their brain and spinal cord were rapidly removed and placed in 4% paraformaldehyde for 24 hours, washed with PBS and placed in 30% sucrose for 24 hours, and then places in PBS at 4°C until further analysis. For myelin basic protein (MBP), glial fibrillary acidic protein (GFAP) and ionized calcium-binding adapter protein 1 (Iba1) immunostaining, brain sections were first washed in PBS to remove excess fixative and then incubated in 0.5% H_2O_2 for 15 min to quench tissue peroxidase activity. Sections were then briefly rinsed in PBS until bubble formation ceased. Subsequently, the sections were incubated in Triton-X-100 and PBS for 45 min to permeabilize the tissue to increase the penetration of antibodies. Subsequently, sections were incubated in the same buffered solution containing blocking serum (10% normal horse

serum) before they were incubated with antibodies against rabbit MBP (Abcam, MA; 1:1000), mouse GFAP (Abcam, MA; 1:1000) or rabbit Iba1 (WAKO, Japan; 1:1000) for 24 hours at 4°C. Primary antiserum dilutions were made in 1% normal horse serum in PBS containing 0.08% sodium azide and 0.02% Kodak Photo-Flo. After thorough rinsing in PBS and Triton X-100, sections were incubated in a solution of biotinylated donkey anti-rabbit IgG or donkey anti-rat IgG for 2 hours (1:200, Jackson Immunoresearch, PA). The sections were then rinsed in PBS and incubated in Streptavidin-peroxidase conjugate (ABC: 1:100 dilution Vector lab, CA) for one hour at room temperature. Afterwards, sections were rinsed in two changes of buffered saline for 5 minutes each, briefly rinsed in Tris–HCl and developed in diaminobenzidine (DAB; 0.03% H_2O_2 + 5 mg DAB), which produced a brown reaction product. The sections were mounted onto slides, air dried on a slide warmer at 50°C for 5 min, and mounted in DPX medium (Sigma).

Quantification of immunoreactivity

The immune complex was visualized with DAB and stained cells were detected by the presence of distinct staining using a positive pixel count algorithm that quantifies the amount of a specific stain on an Aperio whole slide scanner image using Imagescope software (Aperio-Leica Microsystems Inc., Buffalo Grove, IL). Briefly, the brown color of DAB is specified (range of hues and saturation) with three intensity ranges (weak, positive, and strong) for pixels that satisfy the color specification; the algorithm counts the number and intensity sum in each intensity range, along with three additional quantities: average intensity, ratio of strong/total number, and average intensity of weak positive pixels. The algorithm was set with default input parameters when first selected; these inputs were pre-configured for brown color quantification in the three intensity ranges (0-100, 101-175 and 176-220). Stained pixels that did not fall into the positive-color specification were considered negative pixels, and were also counted so that the fraction of positive to total stained pixels could be determined.

RNA Isolation and qPCR Analysis

Mice were anesthetized 23 days post MOG injection with isoflurane prior to cardiac perfusion with 4% paraformaldehyde. The spinal cord was quickly removed and washed in sterile DEPC-PBS. The cervical segments were then dissected into a 1.5 mL tube containing 200 µl Trizol (Invitrogen) and placed on ice. Within 1 hour all samples were homogenized using a sterile plastic micro-homogenizer, and 800 µl Trizol was then added to each sample before storage at −80°C. Alternatively, splenocytes were isolated and equal amounts of cells were suspended in 1 ml Trizol. Total RNA was isolated according to manufacturer's instructions (Trizol Reagent, Invitrogen) reverse transcription (RT) was performed using oligoDT primers and SSIII reverse transcriptase (Invitrogen) to convert mRNA into cDNA. This was followed by qRT-PCR using SYBR Green Master Mix (Invitrogen) on a MJ Research PTC-200 instrument and analyzed using the relative method. All spinal cord samples were normalized using UBC and B2M prior to comparison with the control condition. All splenocyte samples were normalized to B2M and RPLP0 prior to comparison with the control condition.

TNFα ELISA

Mice were anesthetized 23 days post MOG injection with isoflurane and blood was drawn directly from the heart into a lithium heparin tube (BD Microtainer). TNFα concentration in blood samples was determined using a mouse TNFα ELISA kit (R&D systems MTA00B).

Statistical analysis

Results are expressed as mean and S.E.M. of the indicated number of animals. Statistical comparisons by Chi-squared test (χ^2-test) were performed using Excel. The correlation between the clinical score and ventricular volumes measured by MRI was calculated by linear regression and the changes in clinical score in response to each drug treatment over time were tested by two-way analysis of variance (ANOVA) followed by the Bonferroni post hoc test. This analyses were performed using the Prism software package (Graphpad Software, San Diego, CA, USA).

Results

Combination treatment with lenalidomide and nanoceria ameliorates clinical symptoms in EAE mice

In order to test the hypothesis that combined treatment with an anti-inflammatory agent and an antioxidant will result in a greater therapeutic benefit in EAE compared to either treatment alone, we treated mice with the TNFα synthesis inhibitor lenalidomide (25 mg/kg i.p.) and antioxidant cerium oxide nanoparticles (nanoceria; 1.0 mg/kg i.v.). The dose of lenalidomide was chosen based on a previous pharmacokinetic study in mice which showed that similar doses result in therapeutic plasma lenalidomide concentrations of 100 – 1000 ng/ml within 2 hours after i.p. injection (Rozewski et al., 2012). We chose a dose of nanoceria 10-fold lower than that used previously in animal models of CNS inflammation (Heckman et al., 2013), so as to avoid potential adverse effects of nanoceria on peripheral organs (Tseng et al., 2013). The physiochemical properties of nanoceria synthesis are shown in Supplemental Figure 1. High-resolution transmission electron microscopy images revealed round particles with regular morphology and diameters of 3-5 nm. Nanoceria hydrodynamic size and surface charge in double distilled water were 34 ± 6.8 nm and 19.45 ± 1.4 mV, respectively. Ce 3d deconvoluted X-ray photoelectron (e) spectra showed the presence of both Ce^{3+} and Ce^{4+}. Peaks at 898, 888, 882.1, 916.3, 906.3, and 900.4eV corresponding to Ce^{4+} and 885.0, 880.7, 903.6, 899.3 eV corresponding to the Ce^{3+} were identified. Areas under the curves of the peaks were determined and the Ce^{3+}/Ce^{4+} ratios were calculated. The Ce^{3+}/Ce^{4+} ratio for synthesized cerium oxide nanoparticles was 2.57. The surface area of the nanoparticles is one of the key parameters which influences the catalytic activity of the nanoparticles. The surface area was determined using BET and found to be 91 m^2/g.

Lenalidomide was administered once daily intraperitoneally beginning on the day of MOG peptide administration, and nanoceria were delivered intravenously every fourth day beginning on the same day as MOG administration (Figure 1A). Control EAE mice were administered vehicle instead of lenalidomide and nanoceria, and a healthy group of untreated mice that did not receive MOG was also included in the study. Control EAE mice

began to exhibit clinical signs beginning on post-MOG day 11, which continued to increase in severity during the ensuing 5-7 days and remained evident through day 23 (Figure 1B). Lenalidomide treatment alone delayed symptom onset by several days, but did not reduce the maximum severity of symptoms. In contrast, nanoceria treatment did not affect the onset of symptoms or their maximum severity, but did result in significant recovery of function during the last 3 days of the study. EAE mice that received combined treatment with lenalidomide and nanoceria exhibited a dramatic delay in symptom onset, and in the maximum severity of the symptoms with clinical scores significantly lower than for mice in all other EAE groups (Figure 1B). Indeed, whereas 100% of the mice in the vehicle, lenalidomide- and nanoceria-treated groups exhibited a clinical score of more than '1', only 22% of the mice receiving combination therapy had a symptom level greater than 1 on any day (Figure 1C). On day 7 the EAE mice treated with vehicle, nanoceria, and lenalidomide plus nanoceria exhibited reduced performance on the rotarod compared to healthy mice (Figure 1D). On day 17, EAE mice in the vehicle and nanoceria groups exhibited significantly poorer performance on the rotarod compared to healthy mice; lenalidomide treatment significantly attenuated, and combined treatment with lenalidomide and nanoceria prevented, the rotarod performance deficit (Fig. 1D). Towards the end of the study (day 17 and 23), EAE mice in the vehicle-, lenalidomide, and nanoceria-treated groups exhibited significantly lower body weights than mice in the other groups (Figure 1E). In contrast, EAE mice in the combination therapy group maintained body weights similar to healthy mice.

Combination therapy reduces EAE-mediated MRI abnormalities

In the present study we acquired T2-weighted MRI images in 1 mm sections of the brains of mice in all groups. The brains of all mice were scanned 11-13 days and 20-22 days thereafter. Representative images of mice from the different treatment groups are presented in Figure 2A. The correlation between the ventricular volume obtained from the MRI measurements and the neurological score was statistically significant (Figure 2B). The sensitivity of the measurements at each time point was evaluated by determining the ability to detect the differences between the healthy and vehicle-treated EAE control group. For measurements made on days 11-13, the healthy and EAE control groups differed significantly in the ventricular volume, and for the measurements performed on days 20-22, their ventricular volumes did not differ significantly. On days 11-13, mice that received nanoceria did not show significantly smaller ventricular volume compared to the vehicle, whereas lenalidomide-treated mice did (Figure 2C). The mice that received the combined treatment did show significantly smaller ventricular volume compared to vehicle-treated mice at this time point. Additionally, the ventricular volume for mice receiving the combined treatment did not differ significantly from that of the healthy group.

Lenalidomide and nanoceria treatments attenuate myelin loss in EAE mice

On day 23 after MOG administration, all mice were euthanized and their brains removed and processed for immunostaining. As expected, healthy mice exhibited robust MBP immunoreactivity in the corpus callosum, anterior commissure and white matter of the striatum, as well as more diffuse staining throughout the cerebral cortex (Figure 3A). Vehicle-treated EAE mice exhibited a marked reduction of MBP immunoreactivity compared to healthy mice. MBP levels were significantly lower in the vehicle-treated EAE

mice than in EAE mice treated with nanoceria or lenalidomide alone. EAE mice that received combination therapy exhibited significantly more MBP immunoreactivity compared to mice treated with either lenalidomide or nanoceria alone (Figure 3A, B).

Neuroinflammation and glial reactivity is suppressed by lenalidomide – nanoceria combination therapy

Several analogs of thalidomide, including lenalidomide, can suppress inflammation by inhibiting TNFα production (Zhu et al., 2003, Bartlett et al., 2004). To determine whether lenalidomide reduces neuroinflammation in EAE mice, we first measured TNFα levels in serum samples collected from all mice on day 23. As expected, TNFα levels were elevated more than 10-fold in vehicle-treated control EAE mice compared to healthy mice (Figure 4A). EAE mice treated with lenalidomide alone or in combination with nanoceria exhibited significantly lower TNFα levels compared to control EAE mice, whereas nanoceria treatment alone did not reduce TNFα levels significantly. IL-17 levels serum were below the limit of detection in all groups. We next evaluated CNS inflammation by measuring levels of mRNAs encoding IL-17, IFNγ and TNFα in spinal cord tissue. IL-17 mRNA levels were elevated more than 10-fold in vehicle-treated EAE mice compared to healthy mice (Figure 4B). Mice that received combination therapy exhibited significantly lower IL-17 mRNA levels compared to each of the other three EAE groups (Figure 4B). Combined treatment with lenalidomide and nanoceria also significantly suppressed the EAE-induced elevation of spinal cord IFNγ mRNA levels compared to vehicle-treated EAE mice, and compared to EAE mice treated with lenalidomide or nanoceria alone (Figure 4C). The TNFα mRNA level was higher by more than 20-fold in vehicle-treated EAE mice compared to healthy mice; lenalidomide alone and in combination with nanoceria significantly reduced TNFα mRNA levels in EAE mice, whereas nanoceria alone did not (Figure 4D).

Because a hallmark of neuroinflammation is the presence of activated glial cells (astrocytes and microglia) in the affected tissue, we stained brain and spinal cord sections from all mice with antibodies against proteins expressed in high amounts in activated astrocytes (GFAP) and activated microglia (IbaI). As expected, control EAE mice exhibited a robust increase in GFAP immunoreactivity that was evident in major white matter tracts such as the corpus callosum, as well as in adjacent regions of the cerebral cortex (Figure 5A, C). Treatments with lenalidomide, nanoceria and the combination of lenalidomide and nanoceria significantly suppressed astrocyte activation, with the combination therapy providing the greatest reduction in astrocyte activation. Similarly, EAE mice treated with lenalidomide and nanoceria exhibited significantly lower GFAP immunoreactivity in the spinal cord compared to EAE mice treated with vehicle, lenalidomide or nanoceria (Figure 5B, D). Control EAE mice also exhibited greater Iba1 immunoreactivity compared to healthy mice, which was evident in major white matter tracts such as the corpus callosum, as well as in adjacent regions of the cerebral cortex (Figure 6A, C). Mice treated with lenalidomide, nanoceria and the combination of lenalidomide and nanoceria exhibited significantly less microglial activation, with the combination therapy providing the greatest effect (Figure 6A, C). Similarly, combination treatment with lenalidomide and nanoceria resulted in markedly less pronounced Iba1 immunoreactivity in the spinal cord of EAE mice compared to EAE mice treated with vehicle, lenalidomide or nanoceria (Figure 6B, D).

Peripheral immune reaction to MOG is only slightly inhibited by lenalidomide – nanoceria combination therapy

The reduced levels of neuroinflammation in EAE mice treated with lenalidomide plus nanoceria can be due to local inhibition or a consequence of reduced peripheral inflammatory signals. In order to examine this possibility mice were immunized with MOG 33-55 but were not treated with pertussis toxin. Following 10 days of combined treatment with lenalidomide and nanoceria, or vehicle, the mice were sacrificed and their spleens were weighed and the spleen cells dissociated and plated into cell cultures. The spleens of mice treated with lenalidomide plus nanoceria were significantly smaller than the spleens of control mice (Figure 7A, B). RNA was extracted from the splenocytes within the first hour of their dissociation. While, levels of CD86 and IL17 mRNAs in the splenocytes from mice receiving the combination treatment were reduced by 31 and 52 percent, respectively (see Figure 7C), these did not reach statistical significance (P= 0.12 and 0.07, respectively). The percentage of splenocytes expressing CD86 was significantly reduced in response to the combined treatment (Figure 7D). In order to determine if the reduction in CD86 level was maintained *in-vitro* and whether the treatment affected T-cell differentiation to Th17 cells were grown for three days in the presence of MOG, IL23 and either vehicle (cells from vehicle-treated mice) or lenalidomide plus nanoceria (cells from mice treated with lenalidomide plus nanoceria). Spleen cells from mice treated with MOG, lenalidomide and nanoceria exhibited significantly fewer CD86-positive dendritic cells compared to spleen cells from mice treated with MOG and vehicle (Figure 7C, D). There were no significant differences in numbers of MHC-II- or CD11c-positive spleen cells from mice in the two groups. Even after the expansion the levels of Th17 cells were very low in both groups, but significant reduction was observed in response to the combined treatment (Figure 7G) These results suggest that combined treatment with lenalidomide and nanoceria modulates the activation of antigen presenting cells by reducing co-stimulation signals. This may explain the reduction in Th17 cells and in microglia and astrocytes activation but additional mechanisms of action cannot be excluded.

Discussion

We found that combined treatment with lenalidomide and nanoceria largely eliminated the development of clinical symptoms and greatly reduced white matter damage and CNS inflammation in a mouse model of MS. In contrast, treatments with only lenalidomide or only nanoceria were significantly less effective in ameliorating EAE symptoms and neuropathology.

While a therapeutic effect of lenalidomide in an MS model has not been reported previously, thalidomide treatment has been shown to delay EAE symptom onset and reduced symptom severity (Contino-Pepin et al., 2009, Contino-Pepin et al., 2010, Correa et al., 2010). Initially thalidomide was shown to be a TNFα inhibitor, but it has more recently been found to possess additional immune modulatory actions, partly by influencing NF-κB activation and several anti-apoptotic proteins (Vallet et al., 2008). Inhibition of TNFα with anti-TNF antibodies or a chimeric receptor completely prevented EAE development (Klinkert et al., 1997). However, TNFα deficient mice developed EAE, but with a delay in it onset

(Kassiotis et al., 1999), which is similar to our results in the lenalidomide treated mice. In MS patients, anti-TNF therapies such as infliximab worsened symptoms in two MS patients (van Oosten et al., 1996). Moreover anti-TNF therapies that are used for the treatment of other autoimmune disorders may affect myelination, although such actions are poorly understood (Kaltsonoudis et al., 2014). The cause for the variability in anti-TNFα treatment for MS is not clear and probably depends on which type of TNFα is inhibited, soluble or membrane-associated and on which of the two receptors are inhibited. The levels of inhibition and whether it takes place globally or locally in the CNS can also have a major effect on the outcome of TNFα inhibition. In the present study we used a relatively low dose of lenalidomide that was clearly effective in suppressing inflammatory cytokine production in EAE mice as indicated by lower levels of circulating TNFα protein and CNS TNFα mRNA. In addition, lenalidomide suppressed astrocyte and microglia activation. Our MRI analysis revealed that lenalidomide treatment significantly attenuated the ventricular volume increase that is indicative of neuroinflammation in the EAE model at the earlier time point (days 11-13) but not at the later time point (day 20-22). Thus, lenalidomide alone delayed neuroinflammation and symptom onset, but did not prevent the eventual development of clinical symptoms that reached a level of severity similar to vehicle-treated control EAE mice.

Interestingly, we found that although nanoceria treatment did not alter the onset or maximum severity of EAE symptoms, nanoceria-treated mice exhibited a significant improvement in symptoms during the last 5 days of the study. This recovery was not associated with significantly lower levels of neuroinflammatory markers or normalization of MRI abnormalities. This apparent dissociation between presumptive CNS markers of the EAE disease process and clinical symptoms suggests that it may be possible to improve symptoms without reversing neuroinflammatory processes. Consistent with our finding, it was reported that nanoceria treatment attenuates EAE symptoms without affecting the levels of T cell and macrophage infiltration into the CNS (Heckman et al., 2013). Because one established therapeutic mechanism of action of nanoceria is to reduce oxidative stress, it is reasonable to consider that a reduction in cellular oxidative stress is involved in the recovery of function in nanoceria-treated EAE mice.

Compared to EAE mice treated with lenalidomide or nanoceria alone, those that received the combination therapy exhibited lower expression levels of IL17 and CD86 in splenocytes and lower IL-17 and IFNγ in the CNS, and much less damage to myelin. Considerable evidence suggests that IL-17 plays a particularly pivotal role in the propagation of the autoimmune response to oligodendrocyte membrane/myelin proteins and the resulting damage to the axons they insulate (Luchtman et al. 2014, Zepp et al., 2011). IL-17 promotes movement of circulating Th17 lymphocytes and macrophages into the CNS, and within the CNS stimulates microglial activation, thereby exacerbating both humoral and innate immune responses that damage oligodendrocytes and axons. In addition, IL-17 acts synergistically with IFN-γ in the induction of pro-inflammatory cytokines and cell adhesion molecules and in the expression of MHC proteins on oligodendrocytes and axons. Moreover, in response to IL-17, macrophages and microglia generate reactive oxygen species, which contribute to disruption of the blood-brain barrier and the damage to myelin and axons caused by the activated immune cells (Luchtman et al. 2014). Because lenalidomide is a potent inhibitor of

TNFα production, while nanoceria scavenge reactive oxygen species, it is likely that these anti-inflammatory and antioxidant actions mediate the beneficial effects of combined administration of lenalidomide and nanoceria documented in the present study.

MS is a chronic autoimmune disease characterized by periods of motor dysfunction and cognitive impairment, followed by periods of partial recovery. Currently available treatments can reduce the frequency and length of relapse periods, but are not effective in all patients and can have unwanted side-effects (Goldenberg, 2012, Carrithers, 2014). Moreover, there is as yet no treatment that can halt the progressive form of MS. IFN-β and the polypeptide glatiramer acetate are two treatments which are beneficial in many patients with relapsing – remitting MS. Treatment of human T-cells with IFN-β reduces their production of IL-17 and IL-1β while production of the anti-inflammatory cytokine IL-10 increased (Ramgolam et al. 2009), suggesting a general suppressive effect on IL-17-mediated cascades. Glatiramer acetate may counteract inflammation in MS by competing with binding of antigen-presenting cells and suppressing activation of both Th1 and Th17 lymphocytes (Aharoni et al. 2014). It would be of considerable interest to evaluate the relative effectiveness of combinations of IFN-β or glatiramer acetate with lenalidomide and/or nanoceria in EAE mice.

Previous studies demonstrated that nanoceria can cross the blood-brain barrier. It was reported that approximately 0.01% of i.v injected NC accumulate within the brain parenchyma and reduce levels of oxidative stress markers in the brain tissue (Heckman et al., 2013, 2014). Moreover, the induction of EAE involves disrupting the blood-brain barrier with Pertussis toxin and thus it is reasonable to assume that higher amounts of nanoceria will enter into the brain. It is important to note that 10% of the injected nanoceria were reported to accumulate in the spleen (Hirst et al., 2013). Thus, we cannot determine if the beneficial effects of nanoceria resulted from actions in the spleen, blood, brain or any other organ. It will also be important to evaluate the long-term effects of nanoceria treatments as it has been reported that nanoceria can remain in the brain for at least several months which may result in adverse effects (Hardas et al., 2014).

MRI is considered to be a key method for diagnosis and monitoring of MS because of its ability to detect the actual lesions (Calabresi, 2004). Ventricular enlargement measured by MRI has been shown to precede the clinical observation of EAE mice and to coincide with the appearance of pathology in the cerebellum (Lepore et al. 2013). Previous studies have shown that EAE progression can be monitored by changes in the ventricular size (Levy et al. 2010). While the appearance of enlarged ventricles may be associated with the initial inflammatory response, this finding is followed by white matter pathology, motor deficits, weight loss and other manifestations of progressive disease (Ahorani et al. 2013). In the present study we measured the volume of the ventricles and correlated these measurements with the clinical score for each individual mouse; these data showed statistically significant correlations. The dramatic reduction in EAE symptoms in mice treated with lenalidomide plus nanoceria combination therapy indicated that the MRI changes in ventricular volume are predictive of disease severity and therapeutic efficacy.

An increasing number of disorders are treated with multiple drugs that act by different and complementary mechanisms, including cancers and chronic viral infections such as HIV AIDS. Because of the complexity of the cell types and signaling pathways involved, it is unlikely that one drug can alone halt or reverse the disease process in autoimmune neurodegenerative disorders such as MS. Our findings suggest that targeting both inflammatory and oxidative stress pathways simultaneously more effectively counteract the disease process and ameliorate clinical symptoms compared to targeting just one pathway.

Supplementary Material

Refer to Web version on PubMed Central for supplementary material.

Acknowledgement

This research was supported by the Intramural Research Program of the National Insitute on Aging.

References

Aharoni R. Immunomodulation neuroprotection and remyelination - The fundamental therapeutic effects of glatiramer acetate: A critical review. J Autoimmun. 2014; 54:81–92. [PubMed: 24934599]

Aharoni R, Sasson E, Blumenfeld-Katzir T, Eilam R, Sela M, Assaf Y, Arnon R. Magnetic resonance imaging characterization of different experimental autoimmune encephalomyelitis models and the therapeutic effect of glatiramer acetate. Experimental neurology. 2013; 240:130–144. [PubMed: 23153580]

Bartlett JB, Dredge K, Dalgleish AG. The evolution of thalidomide and its IMiD derivatives as anticancer agents. Nature reviews Cancer. 2004; 4:314–322. [PubMed: 15057291]

Calabresi PA. Diagnosis and management of multiple sclerosis. American family physician. 2004; 70:1935–1944. [PubMed: 15571060]

Carrithers MD. Update on Disease-Modifying Treatments for Multiple Sclerosis. Clinical therapeutics. 2014

Chigurupati S, Mughal MR, Okun E, Das S, Kumar A, McCaffery M, Seal S, Mattson MP. Effects of cerium oxide nanoparticles on the growth of keratinocytes, fibroblasts and vascular endothelial cells in cutaneous wound healing. Biomaterials. 2013; 34:2194–2201. [PubMed: 23266256]

Cimini A, D'Angelo B, Das S, Gentile R, Benedetti E, Singh V, Monaco AM, Santucci S, Seal S. Antibody-conjugated PEGylated cerium oxide nanoparticles for specific targeting of Abeta aggregates modulate neuronal survival pathways. Acta biomaterialia. 2012; 8:2056–2067. [PubMed: 22343002]

Contino-Pepin C, Parat A, Patinote C, Roscoe WA, Karlik SJ, Pucci B. Thalidomide derivatives for the treatment of neuroinflammation. ChemMedChem. 2010; 5:2057–2064. [PubMed: 20936622]

Contino-Pepin C, Parat A, Perino S, Lenoir C, Vidal M, Galons H, Karlik S, Pucci B. Preliminary biological evaluations of new thalidomide analogues for multiple sclerosis application. Bioorganic & medicinal chemistry letters. 2009; 19:878–881. [PubMed: 19103485]

Correa JO, Aarestrup BJ, Aarestrup FM. Effect of thalidomide and pentoxifylline on experimental autoimmune encephalomyelitis (EAE). Experimental neurology. 2010; 226:15–23. [PubMed: 20406639]

Das S, Dowding JM, Klump KE, McGinnis JF, Self W, Seal S. Cerium oxide nanoparticles: applications and prospects in nanomedicine. Nanomedicine. 2013; 8:1483–1508. [PubMed: 23987111]

Dowding JM, Dosani T, Kumar A, Seal S, Self WT. Cerium oxide nanoparticles scavenge nitric oxide radical (NO). Chemical communications. 2012; 48:4896–4898. [PubMed: 22498787]

Dowding JM, Song W, Bossy K, Karakoti A, Kumar A, Kim A, Bossy B, Seal S, Ellisman MH, Perkins G, Self WT, Bossy-Wetzel E. Cerium oxide nanoparticles protect against Abeta-induced mitochondrial fragmentation and neuronal cell death. Cell death and differentiation. 2014; 21:1622–1632. [PubMed: 24902900]

Friese MA, Schattling B, Fugger L. Mechanisms of neurodegeneration and axonal dysfunction in multiple sclerosis. Nature reviews Neurology. 2014; 10:225–238. [PubMed: 24638138]

Goldenberg MM. Multiple sclerosis review. P & T : a peer-reviewed journal for formulary management. 2012; 37:175–184. [PubMed: 22605909]

Greer JM. Autoimmune T-cell reactivity to myelin proteolipids and glycolipids in multiple sclerosis. Multiple sclerosis international. 2013; 2013:151427. [PubMed: 24312732]

Hardas SS, Sultana R, Warrier G, Dan M, Wu P, Grulke EA, Tseng MT, Unrine JM, Graham UM, Yokel RA, Butterfield DA. Rat hippocampal responses up to 90 days after a single nanoceria dose extends a hierarchical oxidative stress model for nanoparticle toxicity. Nanotoxicology. 2014; 8(Suppl 1):155–166. [PubMed: 24350865]

Hauser SL, Oksenberg JR. The neurobiology of multiple sclerosis: genes, inflammation, and neurodegeneration. Neuron. 2006; 52:61–76. [PubMed: 17015227]

Heckman KL, DeCoteau W, Estevez A, Reed KJ, Costanzo W, Sanford D, Leiter JC, Clauss J, Knapp K, Gomez C, Mullen P, Rathbun E, Prime K, Marini J, Patchefsky J, Patchefsky AS, Hailstone RK, Erlichman JS. Custom cerium oxide nanoparticles protect against a free radical mediated autoimmune degenerative disease in the brain. ACS Nano. 2013; 7:10582–10596. [PubMed: 24266731]

Heckman KL, Erlichman J, Reed K, Skeels M. Application of mass spectrometry to characterize localization and efficacy of nanoceria in vivo. Adv Exp Med Biol. 2014; 806:561–579. [PubMed: 24952203]

Hirst SM, Karakoti A, Singh S, Self W, Tyler R, Seal S, Reilly CM. Bio-distribution and in vivo antioxidant effects of cerium oxide nanoparticles in mice. Environ Toxicol. 2013; 28:107–118. [PubMed: 21618676]

Jack C, Ruffini F, Bar-Or A, Antel JP. Microglia and multiple sclerosis. Journal of neuroscience research. 2005; 81:363–373. [PubMed: 15948188]

Kaltsonoudis E, Voulgari PV, Konitsiotis S, Drosos AA. Demyelination and other neurological adverse events after anti-TNF therapy. Autoimmunity reviews. 2014; 13:54–58. [PubMed: 24035809]

Kassiotis G, Pasparakis M, Kollias G, Probert L. TNF accelerates the onset but does not alter the incidence and severity of myelin basic protein-induced experimental autoimmune encephalomyelitis. European journal of immunology. 1999; 29:774–780. [PubMed: 10092079]

Klinkert WE, Kojima K, Lesslauer W, Rinner W, Lassmann H, Wekerle H. TNF-alpha receptor fusion protein prevents experimental auto-immune encephalomyelitis and demyelination in Lewis rats: an overview. Journal of neuroimmunology. 1997; 72:163–168. [PubMed: 9042109]

Kotla V, Goel S, Nischal S, Heuck C, Vivek K, Das B, Verma A. Mechanism of action of lenalidomide in hematological malignancies. Journal of hematology & oncology. 2009; 2:36. [PubMed: 19674465]

Lassmann H, van Horssen J, Mahad D. Progressive multiple sclerosis: pathology and pathogenesis. Nature reviews Neurology. 2012; 8:647–656. [PubMed: 23007702]

Lepore S, Waiczies H, Hentschel J, Ji Y, Skodowski J, Pohlmann A, Millward JM, Paul F, Wuerfel J, Niendorf T, Waiczies S. Enlargement of cerebral ventricles as an early indicator of encephalomyelitis. PLos ONE. 2013; 8(8):e72841. [PubMed: 23991157]

Levy H, Assaf Y, Frenkel D. Characterization of brain lesions in a mouse model of progressive multiple sclerosis. Experimental Neurology. 2010; 226:148–158. [PubMed: 20736006]

Neymotin A, Petri S, Calingasan NY, Wille E, Schafer P, Stewart C, Hensley K, Beal MF, Kiaei M. Lenalidomide (Revlimid) administration at symptom onset is neuroprotective in a mouse model of amyotrophic lateral sclerosis. Experimental neurology. 2009; 220:191–197. [PubMed: 19733563]

Sastry PS. Inhibition of TNF-alpha synthesis with thalidomide for prevention of acute exacerbations and altering the natural history of multiple sclerosis. Medical hypotheses. 1999; 53:76–77. [PubMed: 10499831]

Vallet S, Palumbo A, Raje N, Boccadoro M, Anderson KC. Thalidomide and lenalidomide: Mechanism-based potential drug combinations. Leukemia & lymphoma. 2008; 49:1238–1245. [PubMed: 18452080]

van Oosten BW, Barkhof F, Truyen L, Boringa JB, Bertelsmann FW, von Blomberg BM, Woody JN, Hartung HP, Polman CH. Increased MRI activity and immune activation in two multiple sclerosis patients treated with the monoclonal anti-tumor necrosis factor antibody cA2. Neurology. 1996; 47:1531–1534. [PubMed: 8960740]

Zhu YX, Kortuem KM, Stewart AK. Molecular mechanism of action of immune-modulatory drugs thalidomide, lenalidomide and pomalidomide in multiple myeloma. Leukemia & lymphoma. 2013; 54:683–687. [PubMed: 22966948]

Highlights

- Combination therapy with lenalidomide and nanoceria ameliorates EAE symptoms
- Lenalidomide plus nanoceria reduces white matter pathology
- Lenalidomide plus nanoceria suppresses neuroinflammation
- These preclinical findings suggest a novel therapeutic approach for multiple sclerosis

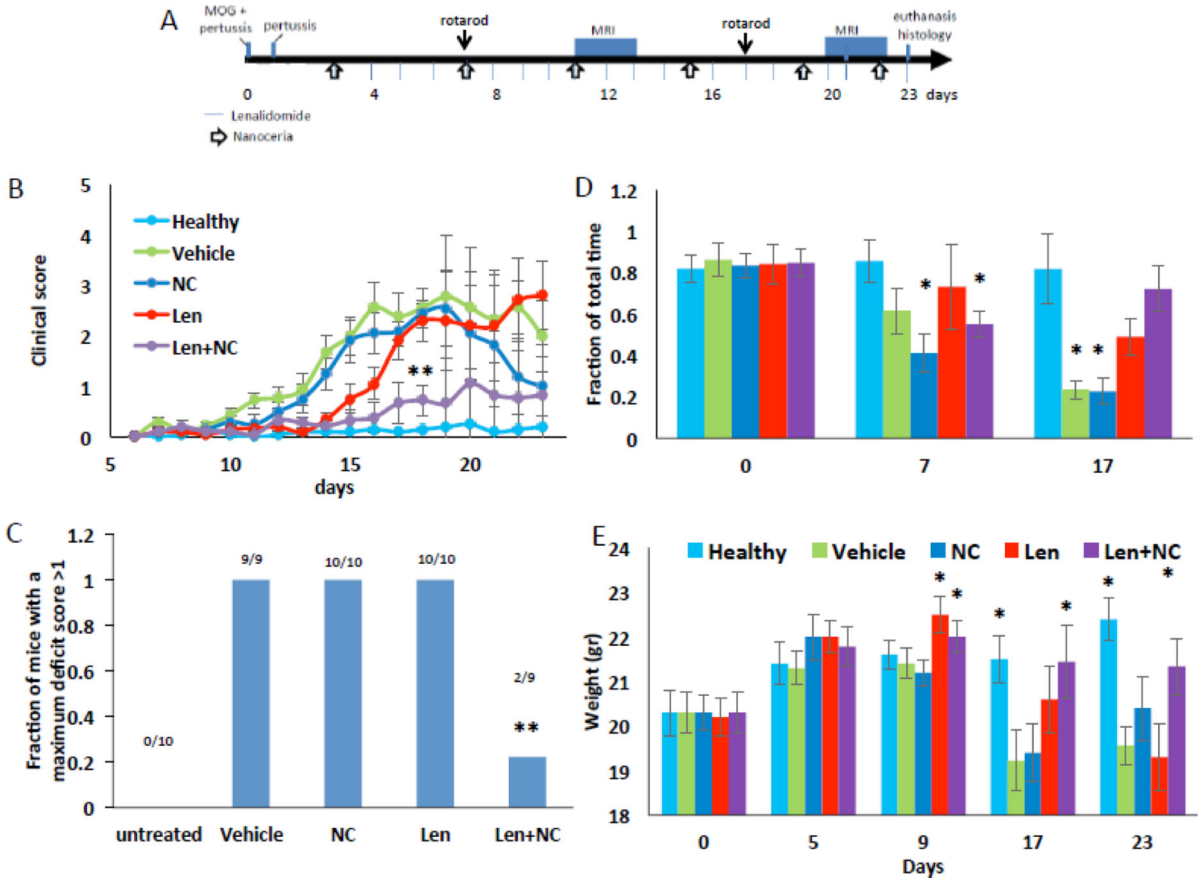

Figure 1.

Combination therapy with lenalidomide and nanoceria ameliorates symptoms in the EAE MS mouse model. **A.** Study design. **B.** Clinical scores. (Len, lenalidomide; NC, nanoceria; Len+NC, lenalidomide + nanoceria). **p<0.01 compared to Vehicle, Len and NC groups. Two-way ANOVA. **C.** Fraction of mice that developed a maximum clinical score greater than 1. **p<0.01 compared to Vehicle, Len and NC groups. Chi-square test. **D.** Rotarod motor performance data from evaluations made on EAE days 7 and 17. *p<0.05 compared to Vehicle, Len and NC groups. ANOVA with Bonferroni post-hoc test. **E.** Animal body weights over the course of the experiment. *p<0.05; **p<0.01. ANOVA with Bonferroni post-hoc test.

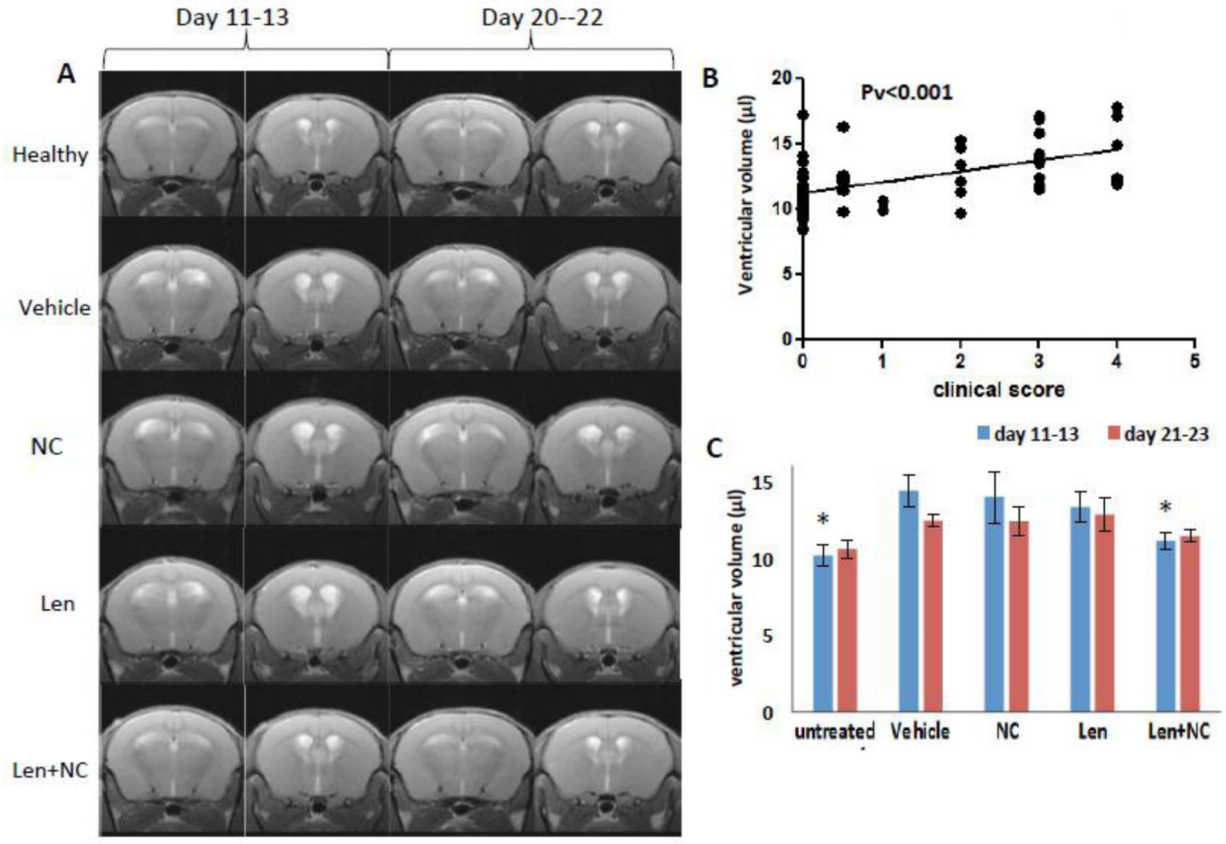

Figure 2.

Lenalidomide and nanoceria combination therapy suppresses enlargement of cerebral ventricles significantly in EAE mice. **A.** Representative T2-weighted images (TE = 30 ms). **B.** Plot of values for ventricle volume and neurological score for each mouse. **C.** Ventricle volumes of mice in the different treatment groups. *p<0.05. ANOVA with Bonferroni post-hoc test.

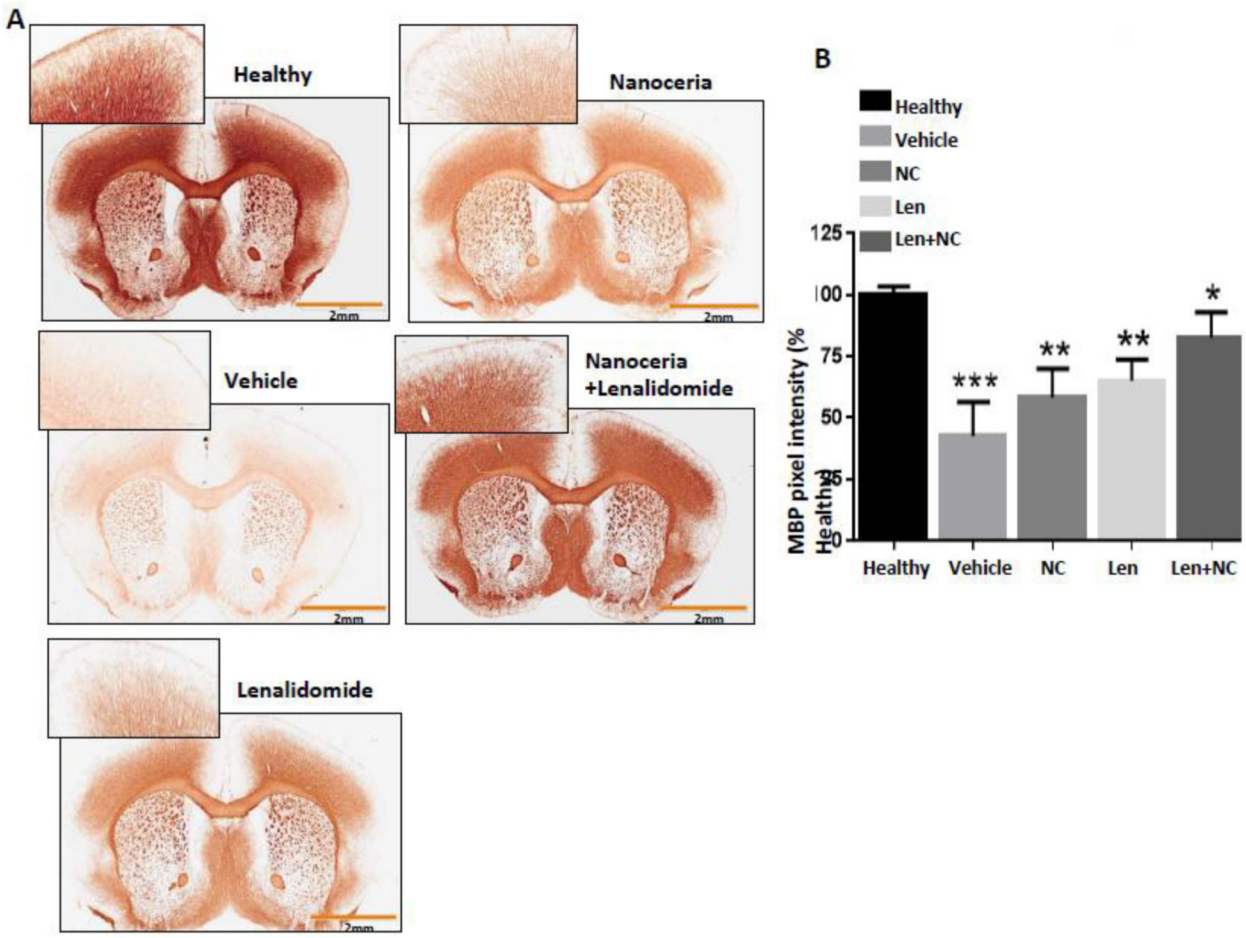

Figure 3.

Myelin is preserved in mice receiving combination therapy with lenalidomide and nanoceria. **A.** Representative images of brain sections immunostained with a myelin basic protein (MBP) antibody. **B.** Quantification of relative MBP staining intensities. Values are the average intensity for entire coronal brain section expressed as a percentage of the average value for healthy mice (mean and SEM of determinations made for 10 healthy mice, 9 vehicle-treated EAE mice, 10 lenalidomide-treated EAE mice, 10 nanoceria-treated EAE mice and 9 lenalidomide + nanoceria-treated EAE mice). *p<0.05; **p<0.01. ANOVA with Bonferroni post-hoc test.

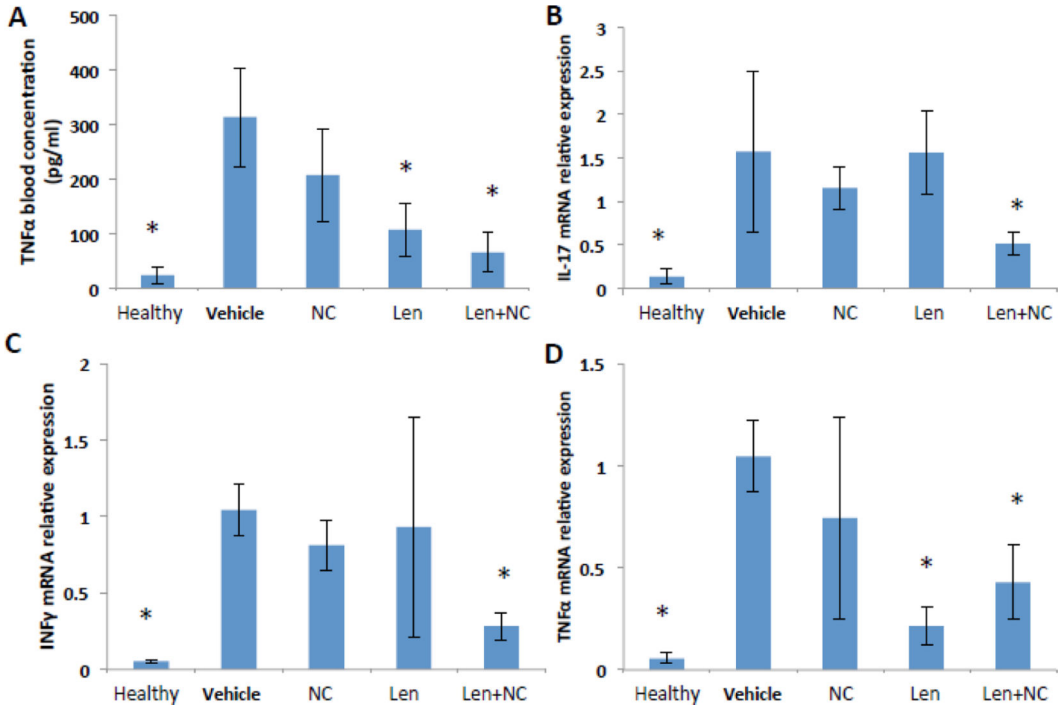

Figure 4.

Combination therapy with lenalidomide and nanoceria suppresses systemic and CNS markers of inflammation in EAE mice. **A.** TNFα protein levels in serum. **B-D.** Relative levels of mRNA encoding the cytokines IL-17 (B), IFN-γ (C) and TNFα (D) in spinal cord tissue samples from mice in the indicated groups. *p<0.05. ANOVA with Bonferroni post-hoc test.

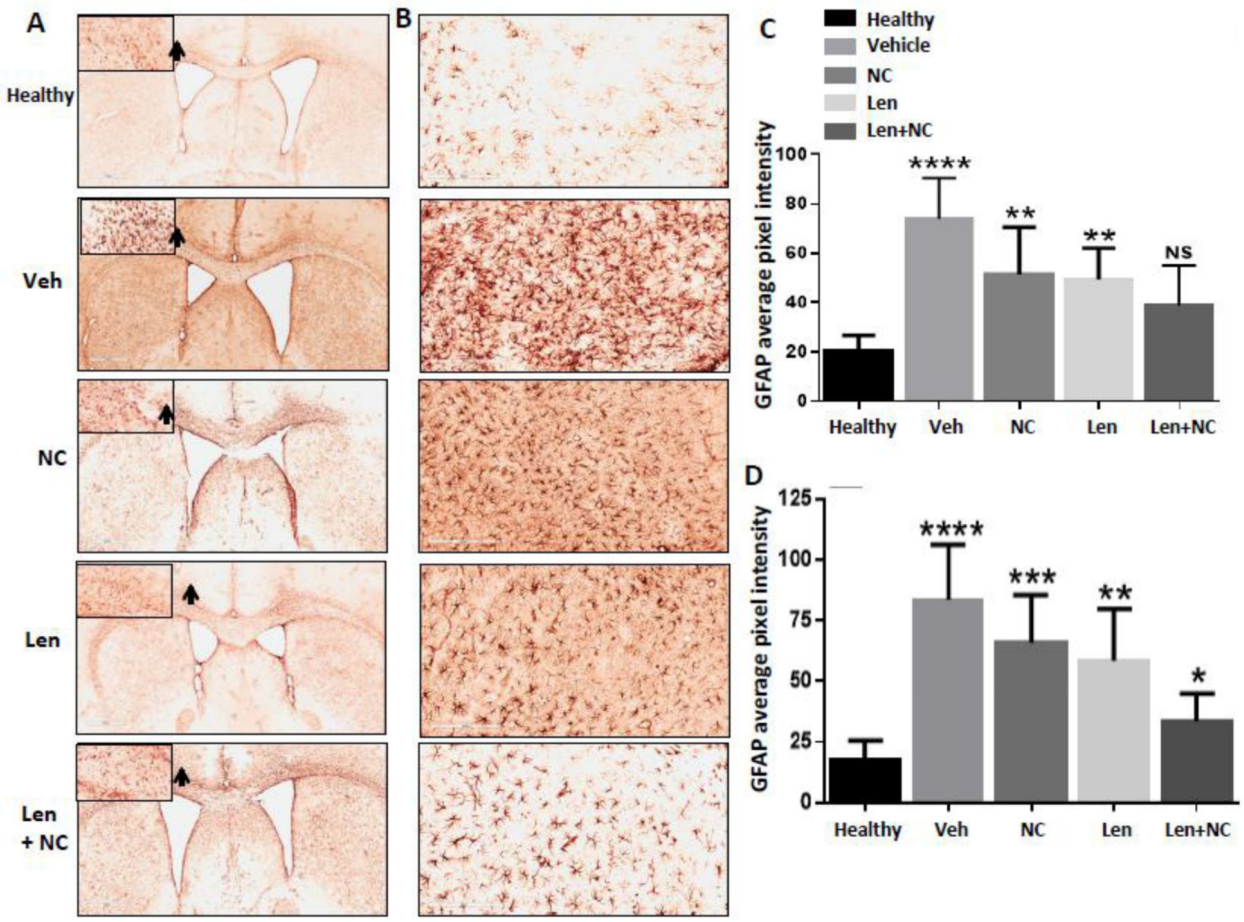

Figure 5.

Combination therapy with lenalidomide and nanoceria suppresses astrocyte activation in the brains of EAE mice. Representative images of GFAP staining in the cortex, striatum and ventricular region (A) and in the lumbar region of the spinal cord (B). **C.** Quantification of GFAP staining from cortex adjacent to the corpus callosum. D. Quantification of GFAP staining from lumbar region of the spinal cord. *p<0.05 ; **p<0.01; ***p<0.001 compared to the value for healthy mice. ANOVA with Bonferroni post-hoc test.

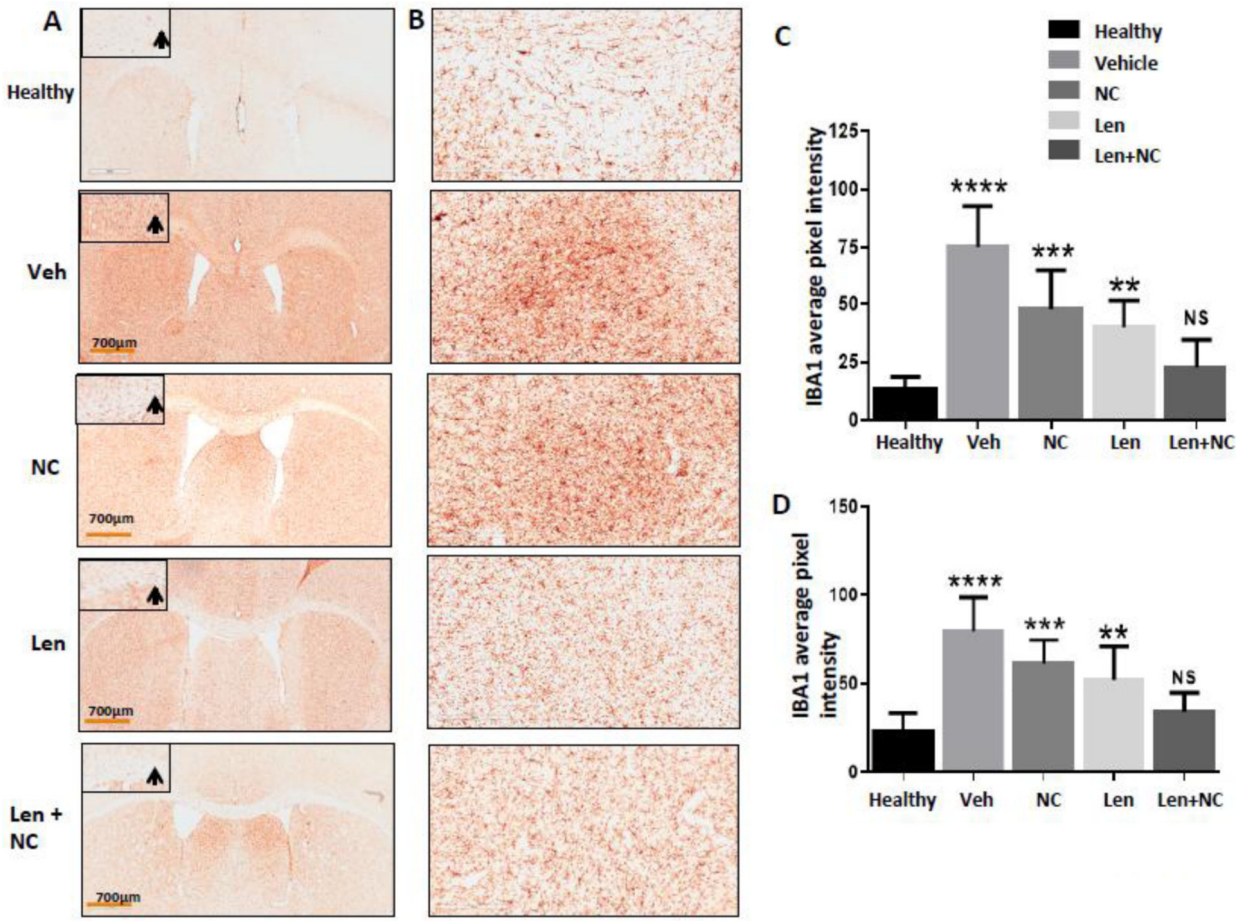

Figure 6.

Combination therapy with lenalidomide and nanoceria suppresses microglial activation in the brains of EAE mice. Representative images of Iba1 staining in the cortex, striatum and ventricular region (A) and in the lumbar region of the spinal cord (B). **C.** Quantification of Iba1 staining from cortex adjacent to the corpus callosum. **D.** Quantification of Iba1 staining from lumbar region of the spinal cord. *p<0.05 ; **p<0.01; ***p<0.001, ****P<0.0001 compared to the value for healthy mice. ANOVA with Bonferroni post-hoc test.

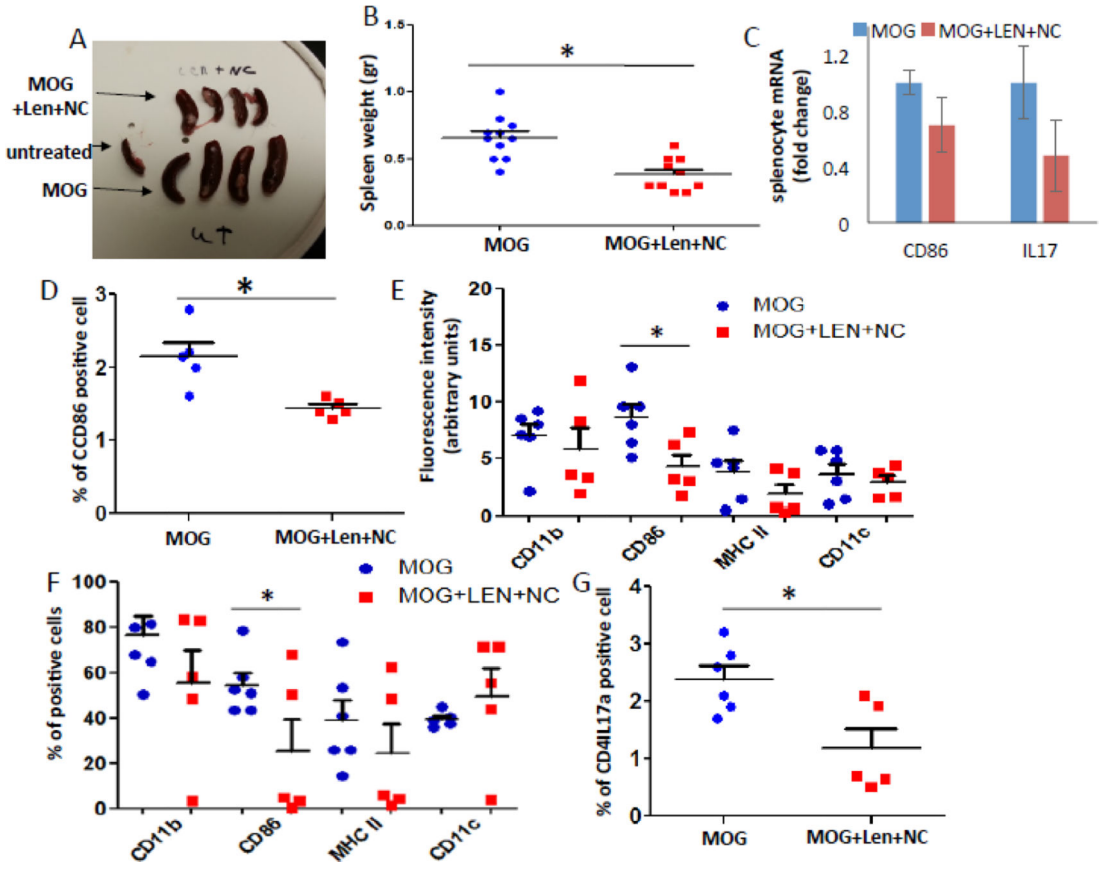

Figure 7.

Combination therapy with lenalidomide and nanoceria inhibits dendritic cell activation in the spleen. **A.** Images of spleens taken from mice immunized with MOG and treated either lenalidomide and nanoceria or vehicle for 10 days. **B.** Spleen weights. C. RNA was isolated from the spleens and the relative levels of mRNA encoding the cytokines IL-17 and coactivation factor CD86 were determined by qRT-PCR. D. Splenocytes were isolated from the spleens and the levels of CD86 expressing cells was measured by FACS. E-G. Splenocytes were cultured for 72 hours in the presence of MOG and IL23. Lenalidomide and nanoceria were added to the culture medium of splenocytes from mice that had received combined treatment, and vehicle was added to the medium of splenocytes from mice that had received vehicle. Cells were stained with antibodies against CD11b, C86, MHC-II and C11c and the average intensity of immunoreactivity for each antigen was quantified (E), the percentage of cells (counted by DAPI) that express each protein was determined (F), and the percentage of T cell that express IL17a was measured by FACS (G). *p<0.05 compared by Student's t test. NC-nanoceria; Lenlenalidomide.